ON A SECOND-ORDER MULTIPOINT FLUX MIXED FINITE ELEMENT METHODS ON HYBRID MESHES[*]

HERBERT EGGER[†] AND BOGDAN RADU[†]

Abstract. We consider the numerical approximation of single-phase flow in porous media by a mixed finite element method with mass lumping. Our work extends previous results of Wheeler and Yotov, who showed that inexact numerical integration together with an appropriate choice of basis leads to some sort of mass lumping which allows eliminating the flux variables locally and reducing the mixed problem to a finite volume discretization for the pressure only. Here we construct second-order approximations for hybrid meshes in two and three space dimensions which, similar to the method of Wheeler and Yotov, allow the local elimination of the flux variables. A full convergence analysis of the method is given for which new arguments and, in part, also new quadrature rules and finite elements are required. The analysis formally also covers approximations of higher order, and third-order elements for triangles and quadrilaterals are presented.

Key words. porous medium equation, mixed finite elements, mass lumping, multipoint flux method

AMS subject classifications. 35F45, 65N30, 76M10

DOI. 10.1137/19M1236862

1. Introduction. We consider the numerical approximation of single-phase flow through a saturated porous medium modeled by the Darcy law and the continuity equation

$$\mathcal{K}^{-1}u + \nabla p = 0 \qquad \text{in } \Omega, \tag{1.1}$$

$$\operatorname{div} u = f \qquad \text{in } \Omega. \tag{1.2}$$

Here Ω is the computational domain, u denotes the flow velocity, p represents the pressure in the fluid, $\mathcal{K}$ is the hydraulic conductivity tensor, and f are the source terms. For ease of notation, we assume that the pressure is known on the whole boundary, i.e.,

$$p = g \qquad \text{on } \partial\Omega, \tag{1.3}$$

but other types of boundary conditions could be considered with minor modifications.

The simulation of problems of the form (1.1)–(1.3) is of practical relevance, e.g., in oil recovery or groundwater hydrology [10, 26]. In such applications, the conductivity $\mathcal{K}$ is usually anisotropic and spatially inhomogeneous, and mixed finite element methods, which have a local conservation property and which perform well for rough and anisotropic coefficients, seem particularly well suited for practical computations.

A major drawback of mixed finite element approximations of (1.1)–(1.3) is that they naturally lead to algebraic saddle point problems that are larger and more difficult to solve than the symmetric positive definite systems obtained by more standard

[†]Department of Mathematics, TU Darmstadt, Darmstadt D-64293, Germany (egger@mathematik.tu-darmstadt.de, bradu@mathematik.tu-darmstadt.de).
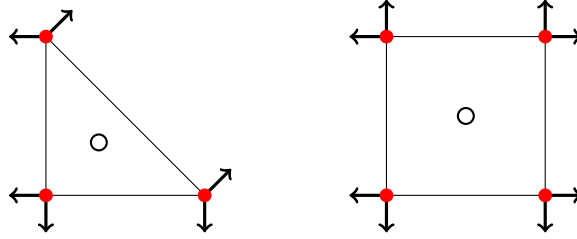
FIG. 1. *Finite elements and quadrature points for the multipoint flux mixed finite element method proposed in* [30]. *For both triangles and quadrilaterals, the local approximation space for velocities is BDM_1, the pressure space is P_0, and the vertex rule is used for numerical integration.*

discretization schemes applied to the reduced problem

$$(1.4) \qquad -\mathrm{div}(\mathcal{K}\nabla p) = f \qquad \text{in } \Omega,$$

$$(1.5) \qquad p = g \qquad \text{on } \partial\Omega,$$

which results from elimination of the velocity variable u in (1.1)–(1.3). An elegant approach that allows keeping the advantages of the mixed finite element approximation and, at the same time, eliminating the difficulties arising from the saddle point structure was proposed by Wheeler and Yotov [30]. They use special quadrature rules and appropriate basis functions for the approximation of the velocity and consider a discrete variational approximation of the following form. Find $(u_h, p_h) \in V_h \times Q_h$ such that

$$(1.6) \qquad (\mathcal{K}^{-1}u_h, v_h)_h - (p_h, \mathrm{div}\, v_h) = \langle g, n \cdot v_h \rangle_{\partial\Omega} \qquad \text{for all } v_h \in V_h \subseteq H(\mathrm{div}, \Omega),$$

$$(1.7) \qquad (\mathrm{div}\, u_h, q_h) = (f, q_h) \qquad \text{for all } q_h \in Q_h \subseteq L^2(\Omega).$$

Here $(\cdot, \cdot)_h$ denotes an approximation of the L^2-scalar product $(\cdot, \cdot)$ over Ω which is obtained by appropriate numerical integration on every element. The degrees of freedom and quadrature points considered in [30] are depicted in Figure 1. A particular choice of basis functions for the spaces V_h and Q_h leads to a linear algebraic system of the form

$$(1.8) \qquad \mathsf{M_h u} - \mathsf{B}^\top \mathsf{p} = \mathsf{g},$$

$$(1.9) \qquad \mathsf{B u} = \mathsf{f},$$

in which the mass matrix $\mathsf{M_h}$ for the velocity variable is block diagonal. This allows locally eliminating u from the system, very similar to the continuous level, and obtaining a reduced problem for the pressure variable of the form

$$(1.10) \qquad \mathsf{B M_h^{-1} B^\top p} = \mathsf{f} + \mathsf{B M_h^{-1} g}.$$

By the block diagonal structure, the mass matrix $\mathsf{M_h}$ has a sparse inverse, and therefore the system matrix $\mathsf{B M_h^{-1} B^\top}$ is sparse and has a compact stencil. Since the vector p here represents local cell averages of the pressure, the system (1.10) can be interpreted as a finite volume discretization of the reduced problem (1.3)–(1.4), which is closely related to certain finite difference and finite volume methods based on multipoint flux approximations [1, 23]. Due to this connection, the above approach was called a *multipoint flux mixed finite element method* in [30]; we refer the reader to
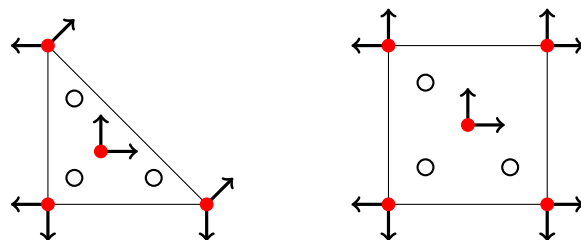
FIG. 2. *Finite elements and quadrature points for the multipoint flux mixed finite element method considered here. The local approximation space for the triangle is the Raviart–Thomas element RT_1, and that for parallelograms is the Brezzi–Douglas–Fortin–Marini element $BDFM_2$. In both cases, the local pressure space is given by P_1, and the vertices and midpoint are chosen as integration points.*

[4, 27, 28] for a detailed discussion of different discretization methods for subsurface flow and their mutual relations.

Besides the algebraic properties mentioned above, the paper [30] also provides a detailed numerical analysis of the approach, including error estimates of first order

$$(1.11) \qquad \|u - u_h\|_{L^2(\Omega)} + \|p - p_h\|_{L^2(\Omega)} \leq Ch,$$

which are optimal in view of the pressure approximation by piecewise constants. By duality arguments, one can even obtain superconvergence for the pressure

$$(1.12) \qquad \|\pi_h^0 p - p_h\|_{L^2(\Omega)} \leq Ch^2$$

provided that the domain Ω is convex and that the conductivity $\mathcal{K}$ is sufficiently smooth. Here $\pi_h^0 : L^2(\Omega) \to P_0(\mathcal{T}_h)$ denotes the projection onto piecewise constants over the mesh. Let us note that, although linear finite elements are used for the velocity approximation, second-order convergence in the velocity is in general not valid, which can be explained by the consistency error introduced by numerical integration in the mass lumping procedure.

The paper [30] covers triangular and tetrahedral grids, as well as quadrilateral meshes consisting of (slightly perturbed) parallelograms. In [21], the extension to affine hexahedral meshes was considered, which required the construction of an extension of the BDDF finite element [7]. The case of general quadrilateral or hexahedral grids, resulting from nonaffine transformations of corresponding reference elements, was treated in [29]. A similar analysis was developed previously for the investigation of related finite difference and finite volume methods [2, 22]. In a recent preprint [3], high-order approximations on affine quadrilateral and hexahedral grids have been considered.

In this paper, we propose and analyze an extension of the theory in [30] to higher orders and explicitly construct second-order approximations on hybrid meshes. In two dimensions, the local approximation spaces and quadrature rules are outlined in Figure 2. Similar to before, the selection of appropriate basis functions allows the systematic reduction to a cell-centered discretization for the reduced problem (1.4)–(1.5). The algebraic problem (1.10) here amounts to an approximation of the pressure with piecewise linear but discontinuous finite elements, and our approach could therefore, in principle, also be interpreted as a particular discontinuous Galerkin approximation.

The accuracy of the quadrature formula depicted in Figure 2 seems to be insufficient at first glance. Indeed, the same arguments of proof as used in [30] would lead to
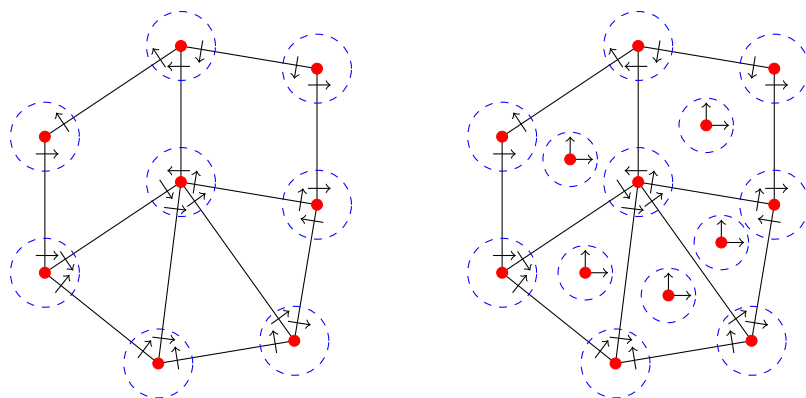
FIG. 3. *Example of a hybrid mesh and distribution of quadrature points and the coupling of degrees of freedom. First-order discretization (left) and second-order discretization (right).*

suboptimal convergence orders. Our analysis, therefore, relies on special properties of the discrete spaces that allow showing the desired convergence rates of second order, i.e.,

$$(1.13) \qquad \|u - u_h\|_{L^2(\Omega)} + \|\pi_h^0(p - p_h)\|_{L^2(\Omega)} + \|p - \widetilde{p}_h^1\|_{L^2(\Omega)} \leq Ch^2,$$

where $\widetilde{p}_h^1$ is a piecewise linear approximation for the pressure which can be obtained, e.g., by the postprocessing strategy of Stenberg [25]. The resulting multipoint flux mixed finite element scheme thus yields the optimal approximation order in both variables. Using duality arguments, we also establish superconvergence estimates for the pressure, which here can be expressed as

$$(1.14) \qquad \|\pi_h^0(p - p_h)\|_{L^2(\Omega)} + \|p - \widetilde{p}_h^2\|_{L^2(\Omega)} \leq Ch^3,$$

where $\widetilde{p}_h^2$ is a piecewise quadratic approximation obtained by local postprocessing.

We develop a general framework for the convergence analysis of mixed finite element methods for arbitrary orders with mass lumping which allows us to treat, in a unified manner, triangular and parallelogram elements in two dimensions as well as tetrahedrons, affine prisms, and parallelepipeds in three dimensions. Our analysis also covers hybrid meshes consisting of different element types; see Figure 3 for a sketch. Appropriate finite elements of second order are constructed explicitly for different element types in two and three space dimensions, and third-order elements for triangles and quadrilaterals are briefly discussed to illustrate the possible extension to higher orders.

Let us note that the results presented in this paper are also of particular relevance for the numerical solution of wave propagation problems, where mass lumping is required to allow for an efficient realization of explicit time stepping schemes. Related mass lumping strategies have been developed for rectangular and simplicial elements in [13] and for Maxwell's equations in [16, 17]; we refer the reader to [12] for an overview. In [14], we provided a full convergence analysis for a mixed finite element approximation of the acoustic wave equation with mass lumping based on the method of Wheeler and Yotov [30].

The remainder of the manuscript is organized as follows. In section 2, we introduce our notation and some basic assumptions that guarantee the well-posedness of the

problem. In section 3, we then present a general framework for the analysis of mixed finite element approximations and summarize basic properties, such as existence and stability. In section 4, we then establish the improved convergence rates (1.13)–(1.14) and also higher-order estimates under some general assumptions. Appropriate second-order finite elements and quadrature rules for different element types in two and three space dimensions are discussed in section 5, and some numerical results are presented for illustration in section 6, including a comparison with the standard mixed finite element method. In the final section, we briefly compare with other methods. Moreover, we discuss the basic construction principles underlying our approach and illustrate the possible extension to higher orders by presenting third-order elements for triangles and quadrilaterals.

2. Preliminaries. In the following, we introduce our notation and some basic assumptions that are required throughout the paper. In addition, we present a general framework for the formulation of mixed finite element approximations with mass lumping.

2.1. Problem data, function spaces, and well-posedness. Throughout the presentation, Ω denotes a bounded Lipschitz domain in two or three space dimensions. In order to ensure the well-posedness of problem (1.1)–(1.3), we assume that $\mathcal{K} \in L^\infty(\Omega)^{d \times d}$ and that $\mathcal{K}(x)$ is symmetric and uniformly positive definite, i.e.,

$$(2.1) \qquad \underline{k}|\xi|^2 \le \xi^\top \mathcal{K}(x)\xi \le \overline{k}|\xi|^2,$$

for a.e. $x \in \Omega$ with some constants $0 < \underline{k}, \overline{k} < \infty$. For our convergence analysis, we will later impose additional conditions on Ω and $\mathcal{K}$ as required.

We denote by $L^p(\Omega)$ and $W^{k,p}(\Omega)$ the usual Lebesgue and Sobolev spaces, and we write $H^k(\Omega) = W^{k,2}(\Omega)$ for ease of notation. The scalar product and norm of $L^2(\Omega)$ are denoted by $(\cdot, \cdot)$ and $\| \cdot \|_{L^2}$. We further define $H(\mathrm{div}, \Omega) = \{u \in L^2(\Omega)^d :$ $\mathrm{div}\, u \in L^2(\Omega)\}$ and denote by $\|u\|_{H(\mathrm{div},\Omega)} = (\|u\|_{L^2(\Omega)}^2 + \|\mathrm{div}\, u\|_{L^2(\Omega)}^2)^{1/2}$ the natural norm for this space. Similar notation is used for the norm of other spaces.

We use C to denote generic constants that may depend on Ω or the polynomial degree of approximation but that are independent of the mesh size and the problem data.

Let us recall some well-known results concerning the analysis of our model problem.

LEMMA 2.1. *For any $f \in L^2(\Omega)$ and $g \in H^{1/2}(\partial\Omega)$, there exists a unique solution $u \in H(\mathrm{div}, \Omega)$, $p \in H^1(\Omega)$ of problem (1.1)–(1.3) and*

$$\|u\|_{H(\mathrm{div})} + \|p\|_{H^1(\Omega)} \le C(\|f\|_{L^2(\Omega)} + |g|_{H^{1/2}(\partial\Omega)}).$$

Proof. Problem (1.1)–(1.3) is equivalent to the reduced problem (1.3)–(1.4), for which existence of a unique solution $p \in H^1(\Omega)$ follows from the Lax–Milgram theorem. Via (1.1), one can recover the velocity field $u = -\mathcal{K}\nabla p \in L^2(\Omega)^d$, and by inserting this into (1.2), one can then deduce that $u \in H(\mathrm{div}, \Omega)$. $\square$

Remark 2.2. On bounded Lipschitz domains, one has $p \in W^{1,p}(\Omega)$ for some $p > 2$ whenever $\mathcal{K}$ is uniformly bounded and elliptic and g is sufficiently smooth; see [20]. Note that by the trace theorem, $g = p|_{\partial\Omega} \in W^{1-1/p,p}(\partial\Omega)$ is a necessary condition. Hence, $u \in L^p(\Omega)^d$, which allows defining normal traces $n \cdot u$ of the velocity along sufficiently smooth $(d-1)$-dimensional manifolds; see [5, section 2.5] for details.

By standard arguments, one can further show the following statement.

LEMMA 2.3. *Under the assumptions of Lemma* 2.1, *the solution of problem* (1.1)–(1.3) *corresponds to the unique solution* $u \in H(\mathrm{div}, \Omega)$, $p \in L^2(\Omega)$ *of the variational problem*

$$(2.2) \qquad (\mathcal{K}^{-1}u, v) - (p, \mathrm{div}\, v) = \langle g, n \cdot v \rangle_{\partial\Omega} \qquad \forall\, v \in H(\mathrm{div}, \Omega),$$

$$(2.3) \qquad (\mathrm{div}\, u, q) = (f, q) \qquad \forall\, q \in L^2(\Omega).$$

The key for establishing the existence of a unique solution $u \in H(\mathrm{div}, \Omega)$ to the variational problem (2.2)–(2.3) via Brezzi's splitting theorem [5, 6] is the surjectivity of the divergence operator, which we state here for later reference.

LEMMA 2.4. *For any* $q \in L^2(\Omega)$, *there exists a function* $v \in H(\mathrm{div}, \Omega)$ *such that* $q = \mathrm{div}\, v$ *and* $\|v\|_{H(\mathrm{div}, \Omega)} \leq C\|q\|_{L^2(\Omega)}$ *with* C *depending only on* Ω. *Moreover, one can choose* $v \in H(\mathrm{div}, \Omega) \cap L^p(\Omega)^d$ *with* $p > 2$ *and such that*

$$\|v\|_{H(\mathrm{div}, \Omega)} + \|v\|_{L^p(\Omega)} \leq C\|q\|_{L^2(\Omega)}.$$

The second assertion follows from the arguments in Remark 2.2 and is used to prove discrete variants of Lemma 2.4; see, e.g., [5, section 2.5] for details.

3. Mixed finite element discretization. We now introduce our notation and the general form of mixed finite element approximations that will be considered in the rest of the paper.

3.1. Mesh. Let $\mathcal{T}_h = \{T_n : n = 1, \dots, N\}$ denote a geometrically conforming partition of the domain Ω into d-dimensional elements in the sense of [11, 18]. In particular, neighboring elements either share a common vertex, edge, or face. Moreover, we assume that any element $T \in \mathcal{T}_h$ is the image $T = F_T(\widehat{T})$ of one of a finite number of reference elements $\widehat{T} \in \{\widehat{T}_1, \dots, \widehat{T}_M\}$ under an affine mapping

$$(3.1) \qquad F_T(\widehat{x}) = a_T + B_T \widehat{x} \qquad \text{with } a_T \in \mathbb{R}^d,\ B_T \in \mathbb{R}^{d \times d}.$$

A partition $\mathcal{T}_h$ of Ω satisfying the above conditions will simply be called a *mesh* in the the following. We denote by h_T the diameter of the element T and call $h = \max_T h_T$ the global mesh size. To have some control on the shape of the elements, we further require that the mesh $\mathcal{T}_h$ be uniformly shape regular; i.e., there exists $c_\gamma > 0$ such that

$$(3.2) \qquad \|B_T\| \leq c_\gamma h_T \qquad \text{and} \qquad \|B_T^{-1}\| \leq c_\gamma h_T^{-1},$$

where h_T is the diameter of the element T. Without loss of generality, we further assume that c_γ is chosen such that $c_\gamma^{-1} h_T^d \leq |\det B_T| \leq c_\gamma h_T^d$ holds as well.

Using standard convention, we denote by $W^{k,p}(\mathcal{T}_h) = \{v \in L^2(\Omega) : v|_T \in W^{k,p}(T)\}$ the broken Sobolev spaces over the mesh $\mathcal{T}_h$, and we use $H^k(\mathcal{T}_h) = W^{k,2}(\mathcal{T}_h)$ for abbreviation. Concerning the problem data, we assume in the following that

(A0) $\mathcal{K}$ satisfies the assumptions of section 2 and $\mathcal{K} \in W^{k+1,\infty}(\mathcal{T}_h)^{d \times d}$ for some $k \geq 0$.

As a consequence, $\mathcal{K}$ is piecewise Lipschitz and the evaluation $\mathcal{K}(x)$ is well defined. For $x \in \partial T$, the value of $\mathcal{K}(x)$ is defined as a limit of values from the interior.

3.2. Approximation spaces. Let $P_k(\mathcal{T}_h) = \{v \in L^2(\Omega) : v|_T \in P_k(T)\}$ be the space of piecewise polynomials over the mesh $\mathcal{T}_h$ of degree smaller than or equal to k. We assume that the approximation spaces V_h, Q_h in the discrete variational problem (1.6)–(1.7) satisfy

(A1) $V_h \subset P_m(\mathcal{T}_h)^d \cap H(\mathrm{div}, \Omega)$ and $Q_h = \mathrm{div}\, V_h \supset P_k(\mathcal{T}_h)$ for some $k, m \geq 0$. The first assumption and the shape regularity of the mesh will allow us to employ inverse estimates for bounding derivatives of functions $v_h \in V_h$. We denote by $\pi_h : L^2(\Omega) \to Q_h$ the L^2-orthogonal projection onto Q_h, defined by

$$(3.3) \qquad (\pi_h p, q_h) = (p, q_h) \qquad \forall q_h \in Q_h,$$

and use π_h^k to denote the orthogonal projections onto $P_k(\mathcal{T}_h)$ and $P_k(\mathcal{T}_h)^d$, respectively. We further assume having access to a suitable interpolation operator Π_h for the velocity space with the following properties.

(A2) $\Pi_h : H(\mathrm{div}, \Omega) \cap L^p(\Omega)^d \to V_h$, $p > 2$ is a linear and bounded projection operator, i.e., $\|\Pi_h u\|_{H(\mathrm{div})} \leq C \|u\|_{H(\mathrm{div}) \cap L^p}$, satisfying the *commuting diagram* property

$$(3.4) \qquad \mathrm{div}\, \Pi_h v = \pi_h \mathrm{div}\, v \qquad \text{for all } v \in H(\mathrm{div}, \Omega) \cap L^p(\Omega)^d.$$

These assumptions can be used to establish the well-posedness of the discrete variational problem (1.6)–(1.7). In particular, they yield the following discrete variant of Lemma 2.4.

LEMMA 3.1. *Let (A0)–(A2) hold. Then, for any $q_h \in Q_h$, there exists a function $v_h \in V_h$ such that $q_h = \mathrm{div}\, v_h$ and $\|v_h\|_{H(\mathrm{div})} \leq C' \|q_h\|_{L^2(\Omega)}$.*

Proof. By Lemma 2.4, there exists a function $v \in H(\mathrm{div}, \Omega) \cap L^p(\Omega)^d$ such that $\mathrm{div}\, v = q_h$ and $\|\mathrm{div}\, v\| + \|v\|_{L^p} \leq C \|q_h\|$. Then the choice $v_h = \Pi_h v$ together with the properties in assumption (A2) immediately yield the result. $\square$

A variety of particular approximation spaces V_h, Q_h and corresponding interpolation and projection operators Π_h, π_h that satisfy assumptions (A0)–(A2) can be found in the literature [7, 8, 9, 24]; we refer the reader to [5, Chapter 2] and to section 5 for details and examples.

3.3. Quadrature rule. As a final ingredient for the formulation of our method, we need to specify the type of quadrature rules to be used in the definition of the discrete variational problem (1.6)–(1.7). For any $u_h, v_h \in V_h$, let us define

$$(3.5) \qquad (u_h, v_h)_h := \sum_{T \in \mathcal{T}_h} (u_h, v_h)_{h,T} := \sum_{T \in \mathcal{T}_h} \left(|T| \sum_{n=1}^{N_T} (u_h \cdot v_h)(x_{n,T}) w_{n,T} \right),$$

where $(x_{n,T}, w_{n,T})$, $n = 1, \ldots, N_T$ denotes the integration points and weights specifying the local quadrature rules on the element T. Note that the definition naturally applies to scalar and vector valued functions. In order to ensure the well-posedness of the discrete variational problem (1.6)–(1.7) and to prove uniform bounds for the solution, we additionally require that

(A3) all weights $\hat{w}_{n,T}$ be positive and the lumped scalar product $(\cdot, \cdot)_h$ uniformly equivalent to the exact scalar product $(\cdot, \cdot)$ on the discrete velocity space V_h, i.e.,

$$(3.6) \qquad c^{-1}(v_h, v_h) \leq (v_h, v_h)_h \leq c\, (v_h, v_h),$$

for all $v_h \in V_h$ with some generic constant $c > 0$ independent of $\mathcal{T}_h$. By assumption (A0) and condition (2.1), the coefficient matrices $\mathcal{K}(x)$ are uniformly elliptic and bounded from above for all x, and as a consequence, we also obtain

$$(3.7) \qquad \hat{c}^{-1}(v_h, v_h) \leq (\mathcal{K}^{-1} v_h, v_h)_h \leq \hat{c}\, (v_h, v_h)$$

for all discrete functions $v_h \in V_h$ with a constant $\hat{c} > 0$ independent of v_h and V_h. Hence, $(\cdot, \cdot)_h$ and $(\mathcal{K}^{-1}\cdot, \cdot)_h$ define scalar products on V_h that are uniformly equivalent to the standard scalar product of $L^2(\Omega)^d$.

3.4. Discrete variational problem. We next show that the system (1.6)–(1.7) attains a unique solution. For later reference, we here consider a slightly more general problem. Find $(w_h, r_h) \in V_h \times Q_h$ such that

$$(3.8) \qquad (\mathcal{K}^{-1} w_h, v_h)_h - (r_h, \operatorname{div} v_h) = a_h(v_h) \qquad \forall \, v_h \in V_h,$$

$$(3.9) \qquad (\operatorname{div} w_h, q_h) = b_h(q_h) \qquad \forall \, q_h \in Q_h,$$

where $a_h : V_h \to \mathbb{R}$ and $b_h : Q_h \to \mathbb{R}$ are some given linear functionals. Standard arguments for the analysis of mixed variational problems then yield the following result.

LEMMA 3.2. *Let* (A0)–(A3) *hold, and let* $a_h : V_h \to \mathbb{R}$ *and* $b_h : Q_h \to \mathbb{R}$ *be some bounded linear functionals. Then problem* (3.8)–(3.9) *has a unique solution* $w_h \in V_h$, $r_h \in Q_h$ *with*

$$(3.10) \qquad \|w_h\|_{H(\operatorname{div})} + \|r_h\|_{L^2(\Omega)} \le C \left(\sup_{v_h \in V_h} \frac{a_h(v_h)}{\|v_h\|_{H(\operatorname{div})}} + \sup_{q_h \in Q_h} \frac{b_h(q_h)}{\|q_h\|_{L^2(\Omega)}} \right),$$

with a constant C that only depends on the constants in the assumptions.

Proof. It suffices to establish the conditions of Brezzi's splitting theorem [6].
(i) One has $(\operatorname{div} v_h, q_h) \le \|v_h\|_{H(\operatorname{div})} \|q_h\|_{L^2(\Omega)}$ and

$$(\mathcal{K}^{-1} w_h, v_h)_h \le \hat{c} \|w_h\|_{L^2} \|v_h\|_{L^2} \le \hat{c} \|w_h\|_{H(\operatorname{div})} \|v_h\|_{H(\operatorname{div})} \qquad \forall \, w_h, v_h \in V_h;$$

i.e., the bilinear forms of the discrete variational problem (3.8)–(3.9) are uniformly continuous on the spaces $V_h \times Q_h$ and $V_h \times V_h$, respectively.
(ii) Lemma 3.1 implies the discrete inf-sup condition

$$\sup_{v_h \in V_h} \frac{(\operatorname{div} v_h, q_h)}{\|v_h\|_{H(\operatorname{div})}} \ge \beta' \|q_h\|_{L^2(\Omega)} \qquad \text{for all } q_h \in Q_h,$$

with $\beta' > 0$ depending only on the constant from Lemma 3.1.
(iii) By assumption (A1), we know that $\operatorname{div} V_h = Q_h$. The condition $(\operatorname{div} v_h, q_h) = 0$ for all functions q_h therefore implies that $\operatorname{div} v_h = 0$. From assumptions (A0) and (A3), we know that

$$(\mathcal{K}^{-1} v_h, v_h)_h \ge \hat{c}^{-1} (v_h, v_h) = \hat{c}^{-1} \|v_h\|_{L^2(\Omega)}^2 \qquad \forall \, v_h \in V_h.$$

Together with the above considerations, we obtain

$$(\mathcal{K}^{-1} v_h, v_h)_h \ge \alpha' \|v_h\|_{L^2(\Omega)}^2 = \alpha' \|v_h\|_{H(\operatorname{div})}^2$$

for all $v_h \in V_h$ satisfying $(\operatorname{div} v_h, q_h) = 0$ for all $q_h \in Q_h$ and with $\alpha' = \hat{c}^{-1} > 0$. This is the discrete kernel ellipticity condition required for Brezzi's splitting theorem. The assertions of the lemma are then a direct consequence of the results in [6]. $\square$

From Lemma 3.2, one can deduce that for any $f \in L^2(\Omega)$ and $g \in H^{1/2}(\partial\Omega)$, the discrete variational problem (1.6)–(1.7) admits a unique solution $(u_h, p_h) \in V_h \times Q_h$ which can be bounded by the norm of the data, up to uniform constants.

4. Error estimates. Based on assumptions (A0)–(A3), we now present an abstract error analysis for the discrete variational problem (1.6)–(1.7). We start by splitting the error

$$\|u - u_h\|_{L^2(\Omega)} \leq \|u - \Pi_h u\|_{L^2(\Omega)} + \|\Pi_h u - u_h\|_{L^2(\Omega)}, \tag{4.1}$$

$$\|p - p_h\|_{L^2(\Omega)} \leq \|p - \pi_h p\|_{L^2(\Omega)} + \|\pi_h p - p_h\|_{L^2(\Omega)} \tag{4.2}$$

into approximation error and discrete error components. Some mild assumptions on the projection operators Π_h and π_h will be required to bound the approximation errors and the consistency errors introduced by the numerical quadrature.

We now present a general convergence analysis that formally covers arbitrary approximation orders. In section 5, we will discuss in some detail the construction of second-order elements which correspond to setting $k = 1$ in the following results.

4.1. Approximation error. In order to characterize and ensure sufficient approximation properties of the spaces V_h and $\mathcal{Q}_h$, we will assume that

(A4) the projection operators Π_h and π_h are defined locally, i.e., $(\Pi_h v)|_T = \Pi_T v|_T$ and $(\pi_h q)|_T = \pi_T q|_T$ for appropriate operators Π_T and π_T, which satisfy

$$\|\Pi_T u - u\|_{H^\ell(T)} \leq C h_T^{k+1-\ell} \|\nabla^{k+1-\ell} u\|_{L^2(T)} \qquad \text{for } u \in H^{k+1}(T)^d, \tag{4.3}$$

$$\|\pi_T p - p\|_{L^2(T)} \leq C h_T^{k+1} \|\nabla^{k+1} p\|_{L^2(T)} \qquad \text{for } p \in H^{k+1}(T) \tag{4.4}$$

for all $T \in \mathcal{T}_h$ and $0 \leq \ell \leq k+1$ with a uniform constant C.

These conditions, which can be verified by scaling arguments and the Bramble–Hilbert lemma, already allow bounding the approximation errors in the above error splitting.

4.2. Quadrature error. As another ingredient for our convergence analysis, we require that the numerical quadrature be sufficiently accurate. We will assume that

(A5) there exists a subspace $V_h^* \subseteq V_h$ with $Q_h^* := \operatorname{div} V_h^* \supset P_0(\mathcal{T}_h)$ and such that the conditions $v_h \in V_h$ and $\operatorname{div} v_h \in Q_h^*$ already imply $v_h \in V_h^*$. Moreover, the quadrature rule is exact on $P_k(\mathcal{T}_h)^d \times V_h^*$, i.e.,

$$\sigma_h(w_h, v_h^*) := (w_h, v_h^*)_h - (w_h, v_h^*) = 0, \tag{4.5}$$

for all functions $w_h \in P_k(\mathcal{T}_h)^d$ and $v_h^* \in V_h^*$.

We denote by $\sigma_T(w_h, v_h) := (w_h, v_h)_{h,T} - (w_h, v_h)_T$ the corresponding local quadrature error on the element T. As a direct consequence, we obtain the following bound.

LEMMA 4.1. *Let assumptions* (A0)–(A5) *hold with some* $k \geq 0$. *Then, for any function* $u \in H(\operatorname{div}, \Omega) \cap H^{k+1}(\mathcal{T}_h)^d$ *and any* $v_h^* \in V_h^*$, *there holds*

$$|\sigma_h(\mathcal{K}^{-1} \Pi_h u, v_h^*)| \leq C h^{k+1} \|\mathcal{K}^{-1}\|_{W^{k+1,\infty}(\mathcal{T}_h)} \|u\|_{H^{k+1}(\mathcal{T}_h)} \|v_h^*\|_{L^2(\Omega)}. \tag{4.6}$$

Proof. By assumption (A5) and the estimates in (3.7), one can see that

$$\begin{aligned}
\sigma_T(\mathcal{K}^{-1} \Pi_h u, v_h^*) &= \sigma_T(\mathcal{K}^{-1} \Pi_h u - \pi_h^{k+1}(\mathcal{K}^{-1} \Pi_h u), v_h^*) \\
&\leq c h_T^d \|\mathcal{K}^{-1} \Pi_h u - \pi_h^{k+1}(\mathcal{K}^{-1} \Pi_h u)\|_{L^\infty(T)} \|v_h^*\|_{L^\infty(\Omega)} \\
&\leq C h_T^{d+k+1} \|\nabla^{k+1}(\mathcal{K}^{-1} \Pi_h u)\|_{L^\infty(T)} \|v_h^*\|_{L^\infty(\Omega)}.
\end{aligned}$$

Using the product rule of differentiation, we can further estimate

$$\|\nabla^{k+1}(\mathcal{K}^{-1} \Pi_h u)\|_{L^\infty(T)} \leq C' \|\nabla^{k+1} \mathcal{K}^{-1}\|_{L^\infty(T)} \|\nabla^{k+1} \Pi_h u\|_{L^\infty(T)}.$$

By scaling, one can show $h_T^{d/2} \|w_h\|_{L^\infty(T)} \leq c' \|w_h\|_{L^2(T)}$ for $w_h = v_h^*$ and $w_h = \nabla^{k+1} \Pi_h u$. The regularity of $\mathcal{K}^{-1}$ and summation over all elements then yields the result. $\square$

4.3. Estimates for the velocity. We can now already establish the following estimates for the error in the approximation of the velocity field.

LEMMA 4.2. *Let* (A0)–(A5) *hold for some* $k \geq 0$, *and assume that* $u \in H^{k+1}(\mathcal{T}_h)$. *Then*

$$(4.7) \qquad \|u - u_h\|_{L^2(\Omega)} \leq Ch^{k+1}\|u\|_{H^{k+1}(\mathcal{T}_h)}.$$

Moreover, if $\mathrm{div}\, u \in H^{k+1}(\mathcal{T}_h)$, *then* $\|\mathrm{div}(u - u_h)\|_{L^2(\Omega)} \leq Ch^{k+1}\|\mathrm{div}\, u\|_{H^{k+1}(\mathcal{T}_h)}$.

Proof. In view of the error splitting (4.1)–(4.2) and assumption (A4), it remains to estimate the discrete error components $w_h = \Pi_h u - u_h$. Using assumption (A2), we deduce from equations (2.3) and (1.7) that

$$(4.8) \qquad (\mathrm{div}\, \Pi_h u, q_h) = (\pi_h \mathrm{div}\, u, q_h) = (\mathrm{div}\, u, q_h) = (\mathrm{div}\, u_h, q_h)$$

for all $q_h \in Q_h$. Since $Q_h = \mathrm{div}\, V_h$, this implies $\mathrm{div}\, \Pi_h u \equiv \mathrm{div}\, u_h$ and therefore

$$(4.9) \qquad \mathrm{div}\, w_h = \mathrm{div}(\Pi_h u - u_h) = 0.$$

From the variational characterizations (2.2)–(2.3) and (1.6)–(1.7) of the continuous and the discrete solutions, we can thus infer that

$$c\|w_h\|^2_{L^2(\Omega)} \leq (\mathcal{K}^{-1}(\Pi_h u - u_h), w_h)_h = (\mathcal{K}^{-1}(\Pi_h u - u_h), w_h)_h + (\pi_h^k p - p_h, \mathrm{div}\, w_h)$$
$$= (\mathcal{K}^{-1}(\Pi_h u - u), w_h) + \sigma_h(\mathcal{K}^{-1}\Pi_h u, w_h) = a_h(w_h).$$

From (4.9) and assumption (A5), we can further deduce that $w_h \in V_h^*$. Together with assumption (A4) and Lemma 4.1, we then obtain

$$a_h(w_h) \leq C\|\Pi_h u - u\|_{L^2(\Omega)}\|w_h\|_{L^2(\Omega)} + |\sigma_h(\mathcal{K}^{-1}\Pi_h u, w_h)|$$
$$\leq Ch^{k+1}(1 + \|\mathcal{K}^{-1}\|_{W^{k+1,\infty}(\mathcal{T}_h)})\|u\|_{H^{k+1}(\mathcal{T}_h)}\|w_h\|_{L^2(\Omega)}.$$

This immediately implies that

$$\|u - u_h\|_{L^2(\Omega)} \leq \|u - \Pi_h u\|_{L^2(\Omega)} + \|\Pi_h u - u_h\|_{L^2(\Omega)}$$
$$\leq Ch^{k+1}(2 + \|\mathcal{K}^{-1}\|_{W^{k+1,\infty}(\mathcal{T}_h)})\|u\|_{H^{k+1}(\mathcal{T}_h)},$$

which is the desired estimate for the velocity error in L^2. From (4.8) and assumptions (A2) and (A4), we further deduce that

$$\|\mathrm{div}(u - u_h)\|_{L^2(\Omega)} = \|\mathrm{div}\, u - \pi_h \mathrm{div}\, u\|_{L^2(\Omega)} \leq Ch^{k+1}\|\mathrm{div}\, u\|_{H^{k+1}(\mathcal{T}_h)},$$

which yields the estimate for the error in the divergence.   ☐

Remark 4.3. Note that, due to assumption (A1), the velocity error only depends on the approximation properties of the velocity space V_h; see [5] for details.

4.4. Estimates for the pressure. In order to prove optimal error estimates for the pressure, we require that the spaces V_h^* and Q_h^* of assumption (A5) define a stable pairing. We denote by $\pi_h^* : L^2(\Omega) \to Q_h^*$ the L^2-orthogonal projection onto Q_h^*, i.e.,

$$(4.10) \qquad (\pi_h^* p, q_h^*) = (p, q_h^*) \qquad \forall q_h^* \in Q_h^*,$$

and we assume that

(A6) there exists a linear bounded projection operator $\Pi_h^* : H^k(\mathcal{T}_h)^d \cap H(\mathrm{div}, \Omega) \to V_h^*$ such that $\pi_h^* \mathrm{div}\, v = \mathrm{div}\, \Pi_h^* v$ holds for all $v \in H(\mathrm{div}, \Omega) \cap H^k(\mathcal{T}_h)^d$. In addition, the projection operator Π_h^* is defined locally, i.e., $(\Pi_h^* v)|_T = \Pi_T^* v|_T$ for an appropriate operator Π_T^* which satisfies

$$\|\Pi_T^* u - u\|_{L^2(T)} \le C h_T \|\nabla u\|_{L^2(T)} \qquad \text{for } u \in H^1(T)^d$$

for all elements $T \in \mathcal{T}_h$ with a uniform constant C.

Together with the previous estimates for the velocity error, we now obtain the following.

LEMMA 4.4. *Let* (A0)–(A6) *hold with some* $k \ge 0$. *Then*

(4.11) $$\|\pi_h^0(p - p_h)\|_{L^2(\Omega)} + \|\pi_h^*(p - p_h)\|_{L^2(\Omega)} \le C h^{k+1} \|u\|_{H^{k+1}(\mathcal{T}_h)}.$$

Proof. By assumptions (A5) and (A6), we have $\pi_h^*(p - p_h) = \mathrm{div}\, v_h^*$ for some $v_h^* \in V_h^*$ with bound $\|v_h^*\|_{H(\mathrm{div})} \le C^* \|\pi_h^*(p - p_h)\|_{L^2(\Omega)}$; compare with Lemma 3.2. Using the variational equations (2.2) and (1.6) as well as assumption (A6), we further deduce that

$$
\begin{aligned}
\|\pi_h^*(p - p_h)\|_{L^2(\Omega)}^2 &\le (\pi_h^*(p - p_h), \mathrm{div}\, v_h^*) = (p - p_h, \mathrm{div}\, v_h^*) \\
&= (\mathcal{K}^{-1}(\Pi_h u - u_h), v_h^*)_h + (\mathcal{K}^{-1}(\Pi_h u - u), v_h^*) - \sigma_h(\mathcal{K}^{-1}\Pi_h u, v_h^*) \\
&\le C h^{k+1} \|u\|_{H^{k+1}(\mathcal{T}_h)} \|v_h^*\|_{L^2(\Omega)}.
\end{aligned}
$$

In the last step, we employed the equivalence of norms provided by (A3), the bounds for the coefficients, the estimates for the approximation error in Lemma 4.2, the improved estimate for the quadrature error in Lemma 4.1, and the previous estimate for the discrete velocity error. The estimate for $\|\pi_h^*(p - p_h)\|_{L^2(\Omega)}$ is now obtained by the stability estimate $\|v_h^*\|_{L^2(\Omega)} \le \|v_h^*\|_{H(\mathrm{div})} \le \beta^{-1} \|\pi_h^*(p - p_h)\|_{L^2(\Omega)}$ in assumption (A5). Since $P_0(\mathcal{T}_h) \subset Q_h^*$ by assumption (A1), we further deduce that $\|\pi_h^0(p - p_h)\|_{L^2(\Omega)} \le \|\pi_h^*(p - p_h)\|_{L^2(\Omega)}$, which completes the proof. $\square$

4.5. Superconvergence for the pressure. As a last step, we now show that even an additional order of convergence for the pressure can be obtained by a duality argument under the assumption that the domain Ω is convex and that $\mathcal{K}$ is globally smooth.

LEMMA 4.5. *Let* (A0)–(A6) *hold with* $k \ge 0$, *and let* Ω *be convex and* $\mathcal{K} \in W^{1,\infty}(\Omega)$. *Then*

$$\|\pi_h^0(p - p_h)\|_{L^2(\Omega)} + \|\pi_h^*(p - p_h)\|_{L^2(\Omega)} \le C h^{k+2} \|u\|_{H^{k+1}(\mathcal{T}_h)}.$$

Proof. Let ϕ denote the solution to the auxiliary problem

$$
\begin{aligned}
\mathrm{div}(\mathcal{K}\nabla\phi) &= \pi_h^*(p - p_h) &&\text{in } \Omega, \\
\phi &= 0 &&\text{on } \partial\Omega,
\end{aligned}
$$

and note that $\|\phi\|_{H^2(\Omega)} \le C \|\pi_h^*(p - p_h)\|_{L^2(\Omega)}$ due to convexity of the domain. Then, by assumption (A6) for the projectors π_h^* and Π_h^*, we obtain

$$
\begin{aligned}
\|\pi_h^*(p - p_h)\|_{L^2(\Omega)}^2 &= (\pi_h^*(p - p_h), \pi_h^* \mathrm{div}(\mathcal{K}\nabla\phi)) = (\pi_h^*(p - p_h), \mathrm{div}(\Pi_h^*(\mathcal{K}\nabla\phi))) \\
&= (\mathcal{K}^{-1}(u - u_h), \Pi_h^*(\mathcal{K}\nabla\phi)) - \sigma_h(\mathcal{K}^{-1}u_h, \Pi_h^*(\mathcal{K}\nabla\phi)) = \text{(i)} + \text{(ii)}.
\end{aligned}
$$

Using that $(u - u_h, \nabla\phi) = -(\text{div}(u - u_h), \phi) = -(\text{div}(u - u_h), \phi - \pi_h^1\phi)$, which follows from (2.3) and (1.7), the approximation properties of assumption (A6), and the estimates of Theorem 4.2, the first term can be further estimated by

$$
\begin{aligned}
\text{(i)} &= (\mathcal{K}^{-1}(u - u_h), \Pi_h^*(K\nabla\phi) - K\nabla\phi) - (\text{div}(u - u_h), \phi - \pi_h^1\phi) \\
&\leq C(\|u - u_h\|_{L^2(\Omega)}\|\Pi_h^*(\mathcal{K}\nabla\phi) - \mathcal{K}\nabla\phi\|_{L^2(\Omega)} + \|\text{div}(u - u_h)\|_{L^2(\Omega)}\|\phi - \pi_h^1\phi\|_{L^2(\Omega)}) \\
&\leq C'h^{k+2}(\|u\|_{H^{k+1}(\mathcal{T}_h)} + \|\text{div}\,u\|_{H^k(\mathcal{T}_h)})\|\phi\|_{H^2(\mathcal{T}_h)} \\
&\leq C''h^{k+2}\|u\|_{H^{k+1}(\mathcal{T}_h)}\|\pi_h^*(p - p_h)\|_{L^2(\Omega)}.
\end{aligned}
$$

For the second term, we can use assumption (A5), similar arguments as in the proof of Lemma 4.1, the regularity of $\mathcal{K}$ and $\mathcal{K}^{-1}$, and inverse estimates to show that locally

$$
\begin{aligned}
\text{(ii)}_T &= \sigma_T(\mathcal{K}^{-1}u_h, \Pi_h^*(\mathcal{K}\nabla\phi)) \\
&\leq Ch_T^{k+2}\|\mathcal{K}^{-1}\|_{W^{k+1,\infty}(T)}\big(\|u_h\|_{H^{k+1}(T)}\|\Pi_h^*(\mathcal{K}\nabla\phi)\|_{H^1(T)}\big) \\
&\leq C'\big(h_T\|\Pi_T u - u_h\|_{L^2(T)} + h_T^{k+2}\|\Pi_T u\|_{H^{k+1}(T)}\big)\|\Pi_h^*(\mathcal{K}\nabla\phi)\|_{H^1(T)}.
\end{aligned}
$$

Using assumption (A4), we can estimate $\|\Pi_T u\|_{H^{k+1}(T)} \leq C\|u\|_{H^{k+1}(T)}$, and by (A6), we show that $\|\Pi_h^*(\mathcal{K}\nabla\phi)\|_{H^1(T)} \leq C\|\mathcal{K}\nabla\phi\|_{H^1(T)}$. From Theorem 4.2, one can further deduce that $\|\Pi_T u - u_h\|_{L^2(\Omega)} \leq Ch_T^{k+1}\|u\|_{H^{k+1}(\mathcal{T}_h)}$. By summation over all elements, we then get

$$
\text{(ii)} \leq Ch^{k+2}\|u\|_{H^{k+1}(\mathcal{T}_h)}\|\pi_h^*(p - p_h)\|_{L^2(\Omega)},
$$

and since $P_0(\mathcal{T}_h) \subset Q_h^*$, we also have $\|\pi_h^0(p - p_h)\|_{L^2(\Omega)} \leq \|\pi_h^*(p - p_h)\|_{L^2(\Omega)}$. □

4.6. Postprocessing for the pressure. In the spirit of Stenberg [25], we now define the following local postprocessing procedure.

PROBLEM 1 (postprocessing for the pressure). *Find $\widetilde{p}_h \in P_{k+1}(\mathcal{T}_h)$ such that for all $T \in \mathcal{T}_h$, there holds*

$$
\begin{aligned}
(4.12) && (\nabla\widetilde{p}_h, \nabla\widetilde{q}_h)_T &= -(\mathcal{K}^{-1}u_h, \nabla\widetilde{q}_h)_T && \forall\widetilde{q}_h \in P_{k+1}(T), \\
(4.13) && (\widetilde{p}_h, q_h^0)_T &= (p_h, q_h^0)_T && \forall q_h^0 \in P_0(T).
\end{aligned}
$$

Note that $\widetilde{p}_h$ can be computed separately on each element T, rendering the method computationally efficient. Following the analysis of [25], we obtain the following bounds.

LEMMA 4.6. *Let (A0)–(A6) hold for some $k \geq 0$. Then*

$$
\begin{aligned}
\|p - \widetilde{p}_h\|_{L^2(T)} &\leq \|p - \pi_h^{k+1}p\|_{L^2(T)} + \|\pi_h^0(p - p_h)\|_{L^2(T)} \\
&\qquad + Ch_T(\|u - u_h\|_{L^2(T)} + \|\nabla(\pi_h^{k+1}p - p)\|_{L^2(T)}).
\end{aligned}
$$

Proof. For convenience of the reader, we recall the basic steps of the derivation of this result. By the triangle inequality, one obtains

$$
\begin{aligned}
\|p - \widetilde{p}_h\|_{L^2(T)} &\leq \|p - \pi_h^{k+1}p\|_{L^2(T)} + \|\pi_h^{k+1}p - \widetilde{p}_h\|_{L^2(T)} \\
&\leq \|p - \pi_h^{k+1}p\|_{L^2(T)} + \|\pi_h^0(\pi_h^{k+1}p - \widetilde{p}_h)\|_{L^2(T)} + \|(id - \pi_h^0)(\pi_h^{k+1}p - \widetilde{p}_h)\|_{L^2(T)} \\
&= \text{(i)} + \text{(ii)} + \text{(iii)}.
\end{aligned}
$$

The first term already appears in the final estimate. For the second, observe that

$$\text{(ii)} = \|\pi_h^0(\pi_h^{k+1}p - \widetilde{p}_h)\|_{L^2(T)} = \|\pi_h^0(p - p_h)\|_{L^2(T)},$$

where we used the properties of the L^2 projections and (4.13). By the optimality of the L^2 projection and the Poincaré inequality, the third term can be estimated by

$$\text{(iii)} = \|(id - \pi_h^0)(\pi_h^{k+1}p - \widetilde{p}_h)\|_{L^2(T)} \leq Ch_T\|\nabla(\pi_h^{k+1}p - \widetilde{p}_h)\|_{L^2(T)}.$$

Using (2.2), we obtain for $\widetilde{q}_h = \pi_h^{k+1}p - \widetilde{p}_h$ that

$$\begin{aligned}
\|\nabla\widetilde{q}_h\|_{L^2(T)}^2 &= (\nabla(\pi_h^{k+1}p - \widetilde{p}_h), \nabla\widetilde{q}_h)_T \\
&= (\nabla(\pi_h^{k+1}p - p), \nabla\widetilde{q}_h)_T + (\mathcal{K}^{-1}(u - u_h), \nabla\widetilde{q}_h)_T \\
&\leq \left(\|\nabla(\pi_h^{k+1}p - p)\|_{L^2(T)} + C\|u - u_h\|_{L^2(T)}\right)\|\nabla\widetilde{q}_h\|_{L^2(T)}.
\end{aligned}$$

Dividing by $\|\nabla\widetilde{q}_h\|_{L^2(T)}$ yields the estimate for the term (iii). The assertion of the lemma now follows by combination with the previous estimates. $\square$

By combination of the previous estimates, we now obtain the following conclusion.

LEMMA 4.7. *Let* (A0)–(A6) *hold with* $k \geq 0$. *Then*

$$\|p - \widetilde{p}_h\|_{L^2(\Omega)} \leq Ch^{k+1}(\|u\|_{H^{k+1}(\mathcal{T}_h)} + \|p\|_{H^{k+1}(\mathcal{T}_h)}).$$

If, in addition, Ω *is convex and* $\mathcal{K} \in W^{1,\infty}(\Omega)$, *then*

$$\|p - \widetilde{p}_h\|_{L^2(\Omega)} \leq Ch^{k+2}(\|u\|_{H^{k+1}(\mathcal{T}_h)} + \|p\|_{H^{k+2}(\mathcal{T}_h)}).$$

Proof. By the approximation properties of assumption (A4) and Lemma 4.5, we can estimated the terms on the right-hand side in Lemma 4.6, which yields the result. $\square$

Remark 4.8. In a similar way as in Problem 1, one could construct an approximation $\widetilde{p}_h^k \in P_k(\mathcal{T}_h)$, for which the first estimate of the previous lemma still remains valid. Let us note again that all estimates of this section, in particular also those for the pressure error, only depend on the approximation properties of the velocity space V_h.

4.7. Summary error estimates. For later reference, let us summarize the results of the analysis given in this section in a single theorem.

THEOREM 4.9. *Let* (A0)–(A6) *hold for some* $k \geq 0$. *Then*

$$\begin{aligned}
\|u - u_h\|_{L^2(\Omega)} + \|\pi_h^0(p - p_h)\|_{L^2(\Omega)} &+ \|p - \widetilde{p}_h\|_{L^2(\Omega)} \\
&\leq Ch^{k+1}(\|u\|_{H^{k+1}(\mathcal{T}_h)} + \|p\|_{H^{k+1}(\mathcal{T}_h)}).
\end{aligned}$$

Moreover, if $\operatorname{div} u \in H^{k+1}(\mathcal{T}_h)$, *then* $\|\operatorname{div}(u - u_h)\|_{L^2(\Omega)} \leq Ch^{k+1}\|\operatorname{div} u\|_{H^{k+1}(\mathcal{T}_h)}$. *If, in addition,* Ω *is convex and* $\mathcal{K} \in W^{1,\infty}(\Omega)$, *then*

$$\|\pi_h^0(p - p_h)\|_{L^2(\Omega)} + \|p - \widetilde{p}_h\|_{L^2(\Omega)} \leq Ch^{k+2}(\|u\|_{H^{k+1}(\mathcal{T}_h)} + \|p\|_{H^{k+2}(\mathcal{T}_h)}).$$

Remark 4.10. The results of Theorem 4.9, except the estimate for the divergence, still hold under slightly milder assumptions. We can relax assumption (A1) to just re-

quire $Q_h \supset P_{k-1}(\mathcal{T}_h)$ and the approximation property of the L^2 projection introduced in assumption (A4) to

$$(4.14) \qquad \|\pi_T p - p\|_{L^2(T)} \leq C h_T^k \|\nabla^k p\|_{L^2(T)} \qquad \text{for } p \in H^k(T), \ T \in \mathcal{T}_h.$$

Under these milder conditions, we are still able to show that if div $u \in H^k(\mathcal{T}_h)$, then

$$\|\text{div}(u - u_h)\|_{L^2(\Omega)} \leq C h^k \|\text{div } u\|_{H^k(\mathcal{T}_h)}.$$

The estimates (1.13) and (1.14) presented in the introduction follow from these bounds and Remark 4.8 with $k = 1$ by a suitable choice of approximation spaces and quadrature rules. This will be discussed in detail in the following section.

5. Second-order finite elements. Let us briefly comment on the general setting which is used in two and three space dimensions. We assume that $\mathcal{T}_h = \{T\}$ is a shape-regular conforming mesh and that every element $T \in \mathcal{T}_h$ is the affine image of a reference triangle or square or a reference tetrahedron, cube, or prism, i.e., $F_T(\widehat{T})$ with $F_T(\widehat{x}) = a_T + B_T \widehat{x}$. The subspaces used in our approximations are defined locally by

$$V_h = \{v \in H(\text{div } \Omega) : v|_T \in V_T\} \quad \text{and} \quad Q_h = \{q \in L^2(\Omega) : q|_T \in Q_T\}$$

with local spaces $V_T = \{v = \frac{1}{\det B_T} B_T \widehat{v} \circ F_T^{-1} : \widehat{v} \in \widehat{V}\}$ and $Q_T = \{q = \widehat{q} \circ F_T^{-1} : \widehat{q} \in \widehat{Q}\}$. Additionally, spaces V_h^* and Q_h^* are defined accordingly via mapping from the local spaces $\widehat{V}^*$ and $\widehat{Q}^*$. Only the spaces $\widehat{V}, \widehat{Q}, \widehat{V}^*$, and $\widehat{Q}^*$ on the reference elements will therefore be defined below. The local quadrature rule in all cases is of the form

$$(5.1) \qquad (u, v)_{h,T} = |T| \sum_{l=1}^{N_T} u(F_T(\widehat{r}_l)) \cdot v(F_T(\widehat{r}_l)) \, \omega_l,$$

where $\widehat{r}_l$ and $\widehat{\omega}_l$, $l = 1, \ldots, N_T$ are the quadrature points and weights on the reference element and $|\widehat{T}|$ is the area of the element $\widehat{T}$; compare with (3.5).

In the following, we introduce ansatz spaces for different reference elements and appropriate quadrature rules for which the conditions (A0)–(A6) required for our theoretical results are valid. In addition, we discuss a choice of basis for the spaces $\widehat{V}$ such that the resulting mass matrix for the velocity variable becomes block diagonal; see Figure 3 and the discussion in the introduction. We start with two-dimensional elements.

5.1. Triangles. As quadrature points for the triangle, we use its vertices $\widehat{r}_1 = (0,0)$, $\widehat{r}_2 = (1,0)$, $\widehat{r}_3 = (0,1)$ and the barycenter $\widehat{r}_4 = (\frac{1}{3}, \frac{1}{3})$ together with weights $\omega_1 = \omega_2 = \omega_3 = \frac{1}{12}$ and $\omega_4 = \frac{3}{4}$. Note that the quadrature rule is exact for functions in $P_2(\widehat{T})$. The local function spaces on the reference triangle are defined as

$$\widehat{V} = \text{RT}_1(\widehat{T}), \qquad \widehat{Q} = P_1(\widehat{T}),$$
$$\widehat{V}^* = \text{BDM}_1(\widehat{T}), \qquad \widehat{Q}^* = P_0(\widehat{T}),$$

and we denote by Π_T and Π_T^* the standard interpolation operators for these spaces; for details, we refer the reader to [5, Chapter 2]. For this choice, all our assumptions (A1)–(A6) are valid. Assumption (A5), for instance, can be verified elementwise as follows: For any $v_h \in \text{RT}_1(T)$ with div $v_h \in P_0(T)$, there exists a $v_h^* \in \text{BDM}_1(T)$ such that div $v_h^* = $ div v_h. It then follows from [5, Corollary 2.3.2] that $v_h \in \text{BDM}_1(T)$.

As a basis for the reference element $\widehat{V} = \mathrm{RT}_1(\widehat{T})$, which complies with the quadrature points and thus leads to a block diagonal mass matrix, we choose

$$\Phi_1(x,y) = (2x^2 + xy - x, y^2 + 2xy - y),$$
$$\Phi_2(x,y) = (x^2 + 2xy - x, 2y^2 + xy - y),$$
$$\Phi_3(x,y) = (-x^2 + xy + x - y, y^2 - xy),$$
$$\Phi_4(x,y) = (-2x^2 - xy + 3x + y - 1, -y^2 - 2xy + y),$$
$$\Phi_5(x,y) = (-x^2 - 2xy + x, -2y^2 - xy + x + 3y - 1),$$
$$\Phi_6(x,y) = (x^2 - xy, -y^2 + xy - x + y),$$
$$\Phi_7(x,y) = (xy, y^2 - y),$$
$$\Phi_8(x,y) = (x^2 - x, xy).$$

Note that, as desired, exactly two basis functions are associated to every quadrature point, while all other basis functions vanish at this point; see Figure 2 for an illustration.

5.2. Parallelograms. The quadrature rule on the reference rectangle is again given by its vertices $\widehat{r}_1 = (0,0)$, $\widehat{r}_2 = (1,0)$, $\widehat{r}_3 = (1,0)$, and $\widehat{r}_4 = (0,1)$ and the barycenter $\widehat{r}_5 = (\frac{1}{2}, \frac{1}{2})$ with weights $\omega_i = \frac{1}{12}$ for $1 \le i \le 4$ and $\omega_5 = \frac{2}{3}$. One can verify that this quadrature formula is exact even for functions in $P_3(\widehat{T})$, which seems a bit surprising.

As function spaces on the reference element, we now use

$$\widehat{V} = \widehat{V}^* = \mathrm{BDFM}_2(\widehat{T}), \qquad\qquad \widehat{Q} = \widehat{Q}^* = P_1(\widehat{T}),$$

and we denote by $\Pi_T = \Pi_T^*$ the standard interpolation operator for the BDFM$_2$ space; for details, see [5]. All conditions (A1)–(A6) required for our theory are valid for this choice.

As basis for BDFM$_2(\widehat{T})$ that complies with the above quadrature rule, we choose

$$\Phi_1(x,y) = (2x^2 - 2xy, 0), \qquad\qquad \Phi_2(x,y) = (2x^2 + 2xy - 2x, 0),$$
$$\Phi_3(x,y) = (0, 2y^2 + 2xy - 2y), \qquad\qquad \Phi_4(x,y) = (0, 2y^2 - 2xy),$$
$$\Phi_5(x,y) = (-2x^2 + 2xy + 2x - 2y, 0), \quad \Phi_6(x,y) = (-2x^2 - 2xy + 4x + 2y - 2, 0),$$
$$\Phi_7(x,y) = (0, -2y^2 - 2xy + 2x + 4y - 2), \; \Phi_8(x,y) = (0, -2y^2 + 2xy - 2x + 2y),$$
$$\Phi_9(x,y) = (x^2 - x, 0), \qquad\qquad \Phi_{10}(x,y) = (0, y^2 - y).$$

Note that again exactly two basis functions can be associated to every quadrature point, while all other basis functions vanish at this point. As a consequence, we obtain a block diagonal mass matrix for the velocity variable; see Figure 3 in the introduction.

Let us briefly discuss how our second-order space on parallelograms compares to the spaces proposed in [3]. There, the second-order approximation requires 18 degrees of freedom for $\widehat{V}$ and 9 for $\widehat{Q}$, while our spaces require only 10 for $\widehat{V}$ and 3 for $\widehat{Q}$.

As a next step, we define appropriate finite elements in three space dimensions.

5.3. Tetrahedra. As quadrature points, we again choose the vertices $\widehat{r}_1 = (0,0,0)$, $\widehat{r}_2 = (1,0,0)$, $\widehat{r}_3 = (0,1,0)$, and $\widehat{r}_4 = (0,0,1)$ of the reference tetrahedron and its barycenter $\widehat{r}_4 = (\frac{1}{4}, \frac{1}{4}, \frac{1}{4})$, and we set the weights to $\omega_i = \frac{1}{20}$ for $1 \le i \le 4$ and $\omega_5 = \frac{4}{5}$. Let us note that this quadrature formula is exact for functions in $P_2(\widehat{T})$.
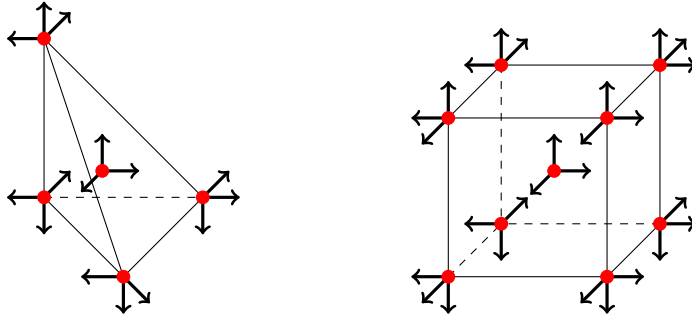
FIG. 4. *Degrees of freedom for the space* $\widehat{V} = RTN_1(\widehat{T})$ *on the tetrahedron (left) and for the new space* $\widehat{V} = \widehat{\mathcal{Q}}_1(\widehat{T})^+$ *on the hexahedron (right). The corresponding quadrature points are depicted by red dots.*

As function spaces on the reference element, we here choose

$$\widehat{V} = \mathrm{RTN}_1(\widehat{T}), \qquad \widehat{Q} = P_1(\widehat{T}),$$
$$\widehat{V}^* = \mathrm{BDDF}_1(\widehat{T}), \qquad \widehat{Q}^* = P_0(\widehat{T}),$$

and we denote by Π_T and Π_T^* the standard interpolation operators for these spaces; see again [5, Chapter 2] for details. All conditions (A1)–(A6) are then valid for this choice.

We next construct an appropriate basis for the space $\widehat{V} = \mathrm{RTN}_1(\widehat{T})$ on the reference element. We start by defining three functions

$$\Phi_{13}(x,y) = (x^2 - x, xy, xz), \quad \Phi_{14}(x,y) = (yx, y^2 - y, yz), \quad \Phi_{15}(x,y) = (zx, zy, z^2 - z)$$

associated to the interior quadrature point and then define 12 additional basis functions for the vertices by

$$
\begin{array}{ll}
\Phi_1(x,y) = (x,0,0) \quad + 2\Phi_{13} + \Phi_{14} + \Phi_{15}, & \Phi_2(x,y) = (0,y,0) \qquad\qquad + \Phi_{13} + 2\Phi_{14} + \Phi_{15}, \\
\Phi_3(x,y) = (0,0,z) \quad + \Phi_{13} + \Phi_{14} + 2\Phi_{15}, & \Phi_4(x,y) = (-y,y,0) \qquad\qquad - \Phi_{13} + \Phi_{14}, \\
\Phi_5(x,y) = (-z,0,z) - \Phi_{13} + \Phi_{15}, & \Phi_6(x,y) = (x+y+z-1,0,0) - 2\Phi_{13} - \Phi_{14} - \Phi_{15}, \\
\Phi_7(x,y) = (0,-z,z) - \Phi_{14} + \Phi_{15}, & \Phi_8(x,y) = (0,x+y+z-1,0) - \Phi_{13} - 2\Phi_{14} - \Phi_{15}, \\
\Phi_9(x,y) = (x,-x,0) + \Phi_{13} - \Phi_{14}, & \Phi_{10}(x,y) = (0,0,x+y+z-1) - \Phi_{13} - \Phi_{14} - 2\Phi_{15}, \\
\Phi_{11}(x,y) = (x,0,-x) + \Phi_{13} - \Phi_{15}, & \Phi_{12}(x,y) = (0,y,-y) \qquad\qquad + \Phi_{14} - \Phi_{15}.
\end{array}
$$

Let us note that exactly three basis functions are associated to every quadrature point, while all other basis functions vanish at this point; see Figure 4. As a consequence, the resulting mass matrix for the velocity variable will be block diagonal.

5.4. Parallelepipeds. The quadrature rule for the reference cube is again defined by its vertices $\widehat{r}_1 = (0,0,0)$, $\widehat{r}_2 = (1,0,0)$, $\widehat{r}_3 = (0,1,0)$, $\widehat{r}_4 = (1,1,0)$, $\widehat{r}_5 = (0,0,1)$, $\widehat{r}_6 = (1,0,1)$, $\widehat{r}_7 = (0,1,1)$, and $\widehat{r}_8 = (1,1,1)$ and its barycenter $\widehat{r}_4 = (\frac{1}{2}, \frac{1}{2}, \frac{1}{2})$ with weights $\omega_i = \frac{1}{24}$ for $1 \le i \le 8$ and $\omega_9 = \frac{2}{3}$. One can verify that this quadrature formula is exact for functions in $P_3(\widehat{T}) \oplus \mathrm{span}\{x^2yz, xy^2z, xyz^2\}$. Now let $\mathcal{Q}_1(\widehat{T})$ denote the space of trilinear functions on the reference hexahedron $\widehat{T}$. As local ansatz spaces for the hexahedron, we then choose

$$\widehat{V} = \widehat{V}^* = \mathcal{Q}_1(\widehat{T})^3 \oplus \mathrm{span}\left\{ \begin{pmatrix} x^2 \\ 0 \\ 0 \end{pmatrix}, \begin{pmatrix} 0 \\ y^2 \\ 0 \end{pmatrix}, \begin{pmatrix} 0 \\ 0 \\ z^2 \end{pmatrix} \right\},$$

and we set $\widehat{Q} = \widehat{Q}^* = \operatorname{div} \widehat{V}$; note that the function xyz is not contained in $\widehat{Q}$. In the usual manner [5], an interpolation operator $\Pi_T = \Pi_T^*$ for $\widehat{V}$ can be defined by

$$\int_e n \cdot (u - \Pi_T u)\, p_1 = 0 \quad \forall p_1 \in P_1(e), e \in \partial T,$$

$$\int_T (u - \Pi_T u)\, p_0 = 0 \quad \forall p_0 \in P_0(T)^3.$$

This operator has the required approximation properties required for our theory and also satisfies the commuting diagram property with the L^2 projection on the space $\widehat{Q} = \widehat{Q}^*$. In summary, the conditions (A1)–(A6) required for our error estimates are valid.

In order to simplify the definition of a basis for $\widehat{V}$, we introduce two auxiliary functions

$$a(x,y,z) = xyz \quad \text{and} \quad b(w) = \tfrac{1}{2} w(w-1).$$

Then the basis for $\widehat{V}$ for the reference element $\widehat{T}$ is defined by the 24 functions

$$\Phi_1 = (a(x, 1-y, z) - b(x), 0, 0), \qquad \Phi_2 = (a(x, y, z) - b(x), 0, 0),$$
$$\Phi_3 = (a(x, y, 1-z) - b(x), 0, 0), \qquad \Phi_4 = (a(x, 1-y, 1-z) - b(x), 0, 0),$$
$$\Phi_5 = -(a(1-x, 1-y, z) - b(x), 0, 0), \qquad \Phi_6 = -(a(1-x, y, z) - b(x), 0, 0),$$
$$\Phi_7 = -(a(1-x, y, 1-z) - b(x), 0, 0), \qquad \Phi_8 = -(a(1-x, 1-y, 1-z) - b(x), 0, 0),$$

$$\Phi_9 = -(0, a(1-x, 1-y, z) - b(y), 0), \qquad \Phi_{10} = -(0, a(x, 1-y, z) - b(y), 0),$$
$$\Phi_{11} = -(0, a(x, 1-y, 1-z) - b(y), 0), \qquad \Phi_{12} = -(0, a(1-x, 1-y, 1-z) - b(y), 0),$$
$$\Phi_{13} = (0, a(1-x, y, z) - b(y), 0), \qquad \Phi_{14} = (0, a(x, y, z) - b(y), 0),$$
$$\Phi_{15} = (0, a(x, y, 1-z) - b(y), 0), \qquad \Phi_{16} = (0, a(1-x, y, 1-z) - b(y), 0),$$

$$\Phi_{17} = -(0, 0, a(1-x, 1-y, 1-z) - b(z)), \quad \Phi_{18} = -(0, 0, a(x, 1-y, 1-z) - b(z)),$$
$$\Phi_{19} = -(0, 0, a(x, y, 1-z) - b(z)), \qquad \Phi_{20} = -(0, 0, a(1-x, y, 1-z) - b(z)),$$
$$\Phi_{21} = (0, 0, a(1-x, 1-y, z) - b(z)), \qquad \Phi_{22} = (0, 0, a(x, 1-y, z) - b(z)),$$
$$\Phi_{23} = (0, 0, a(x, y, z) - b(z)), \qquad \Phi_{24} = (0, 0, a(1-x, y, z) - b(z)),$$

which are associated to the eight vertices, as well as the three basis functions

$$\Phi_{25} = (2b(x), 0, 0), \quad \Phi_{26} = (0, 2b(y), 0), \quad \Phi_{27} = (0, 0, 2b(z))$$

for the barycenter. Note that again exactly three basis functions are associated to every quadrature point, while all other basis functions vanish at this point; see Figure 4. As a consequence, the mass matrix for the velocity variable will be block diagonal.

5.5. Affine prisms. The quadrature points for the reference prism are defined by its vertices $\widehat{r}_1 = (0,0,0)$, $\widehat{r}_2 = (1,0,0)$, $\widehat{r}_3 = (0,1,0)$, $\widehat{r}_4 = (0,0,1)$, $\widehat{r}_5 = (1,0,1)$, and $\widehat{r}_6 = (0,1,1)$ and two additional interior points $\widehat{r}_8 = (\frac{1}{3}, \frac{1}{3}, \frac{1}{3})$ and $\widehat{r}_7 = (\frac{1}{3}, \frac{1}{3}, \frac{2}{3})$. Let us note that, together with the weights $\omega_i = \frac{1}{24}$ for $1 \le i \le 6$ and $\omega_7 = \omega_8 = \frac{3}{8}$, this quadrature formula is exact for functions in $P_1(\widehat{T}) \oplus \operatorname{span}\{1, x, y, z, xz, yz\}$.

The auxiliary space $\widehat{V}^*$ here is spanned by the set of basis functions

$$\Psi_1(x,y) = (xz, 0, 0), \qquad \Psi_2(x,y) = (0, yz, 0),$$
$$\Psi_3(x,y) = (-yz, yz, 0), \qquad \Psi_4(x,y) = ((x+y-1)z, 0, 0),$$
$$\Psi_5(x,y) = (0, (x+y-1)z, 0), \qquad \Psi_6(x,y) = (xz, -xz, 0),$$
$$\Psi_7(x,y) = (x(1-z), 0, 0), \qquad \Psi_8(x,y) = (0, y(1-z), 0),$$

$$\Psi_9(x,y) = (-y(1-z), y(1-z), 0), \qquad \Psi_{10}(x,y) = ((x+y-1)(1-z), 0, 0),$$
$$\Psi_{11}(x,y) = (0, (x+y-1)(1-z), 0), \qquad \Psi_{12}(x,y) = (x(1-z), -x(1-z), 0),$$
$$\Psi_{13}(x,y) = (0, 0, (1-x-y)z), \qquad \Psi_{14}(x,y) = (0, 0, xz),$$
$$\Psi_{15}(x,y) = (0, 0, yz), \qquad \Psi_{16}(x,y) = (0, 0, -(1-x-y)(1-z)),$$
$$\Psi_{17}(x,y) = (0, 0, -x(1-z)), \qquad \Psi_{18}(x,y) = (0, 0, -y(1-z)),$$

and we set $\widehat{Q}^* = \operatorname{div} \widehat{V}^* = P_1(\widehat{T})$ as before. In order to define the space $\widehat{V}$, we enrich the space $\widehat{V}^*$ by an additional six basis functions,

$$\Phi_{19}(x,y) = \tfrac{9}{2}(0, 0, xz^2(1-z)), \qquad \Phi_{20}(x,y) = \tfrac{9}{2}(0, 0, xz(1-z)^2),$$
$$\Phi_{21}(x,y) = 9(xyz(1-x-y), 0, 0), \qquad \Phi_{22}(x,y) = 9(xy(1-z)(1-x-y), 0, 0),$$
$$\Phi_{23}(x,y) = 9(0, xyz(1-x-y), 0), \qquad \Phi_{24}(x,y) = 9(0, xy(1-z)(1-x-y), 0),$$

associated to the two inner quadrature points. Note that

$$\dim\left(\operatorname{span}\{\operatorname{div}\Phi_i\,,\ i = 1\dots 24\}\right) = 10,$$
$$\dim\left(\operatorname{span}\{\operatorname{div}\Phi_i\,,\ i = 19\dots 24\}\right) = \dim\left(\operatorname{span}\{\Phi_i\,,\ i = 19\dots 24\}\right) = 6.$$

This validates (A5) since the six additional basis functions produce pairwise linearly independent divergences. Moreover, the quadrature formula $(\cdot, \cdot)_h$ is exact for $P_1(\widehat{T})^d \times \widehat{V}^*$. In the usual manner [3, 5], one can define appropriate interpolation operators Π_T, Π_T^* for the spaces $\widehat{V}$, $\widehat{V}^*$ such that all conditions (A1)–(A4) and (A6) of our theory are valid.

As a basis for $\widehat{V}$ that complies with the quadrature rule given above, we choose

$$\Phi_1 = \Psi_1 - \Phi_{21}, \qquad \Phi_2 = \Psi_2 - \Phi_{23}, \qquad \Phi_3 = \Psi_3 + \Phi_{21} - \Phi_{23},$$
$$\Phi_4 = \Psi_4 + \Phi_{21}, \qquad \Phi_5 = \Psi_5 + \Phi_{23}, \qquad \Phi_6 = \Psi_6 - \Phi_{21} + \Phi_{23},$$
$$\Phi_7 = \Psi_7 - \Phi_{22}, \qquad \Phi_8 = \Psi_8 - \Phi_{24}, \qquad \Phi_9 = \Psi_9 + \Phi_{22} - \Phi_{24},$$
$$\Phi_{10} = \Psi_{10} + \Phi_{22}, \qquad \Phi_{11} = \Psi_{11} + \Phi_{24}, \qquad \Phi_{12} = \Psi_{12} - \Phi_{22} + \Phi_{24},$$
$$\Phi_{13} = \Psi_{13} - \Phi_{19}, \qquad \Phi_{14} = \Psi_{14} - \Phi_{19}, \qquad \Phi_{15} = \Psi_{15} - \Phi_{19},$$
$$\Phi_{16} = \Psi_{16} + \Phi_{20}, \qquad \Phi_{17} = \Psi_{17} + \Phi_{20}, \qquad \Phi_{18} = \Psi_{18} + \Phi_{20},$$

for the vertices and $\Phi_{19}, \dots, \Phi_{24}$ for the two inner quadrature points. Note that again exactly three basis functions are associated to each quadrature point, while all other basis functions vanish at this point; see Figure 5. As a consequence, we again obtain a block diagonal mass matrix for the velocity variable.

Remark 5.1. For the above choices of reference elements, all assumptions (A1)–(A6) required for our theory are valid. A quick inspection shows that the degrees of freedom of different elements are compatible, such that we can consider hybrid meshes without further considerations. By construction of the basis functions, the mass matrices for the velocity variable will be block diagonal. In summary, we thus obtain a second-order multipoint flux approximation in the spirit of Wheeler and Yotov [30].
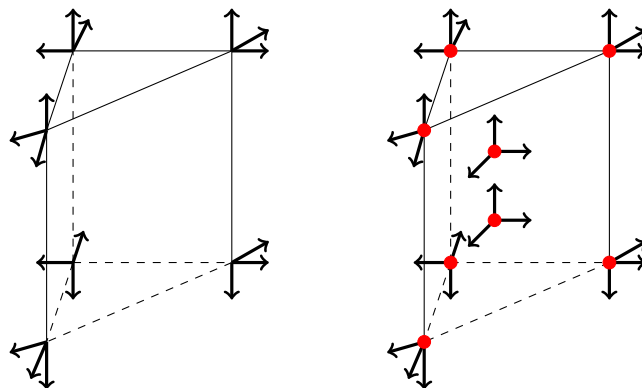
FIG. 5. *Degrees of freedom of the spaces $\widehat{V}^*$ (left) and $\widehat{V}$ (right) by arrows. The quadrature points are depicted by the red dots.*

TABLE 1
Degrees of freedom, relative discretization errors, and estimated orders of convergence (eoc) for the second-order multipoint flux finite element method.

h	DOF u	DOF p	$\frac{\|u-u_h\|}{\|u\|}$	eoc	$\frac{\|p-p_h\|}{\|p\|}$	eoc	$\frac{\|\pi_h^0(p-p_h)\|}{\|\pi_h^0 p\|}$	eoc
2^{-1}	164	84	0.078309	—	0.064026	—	0.033106	—
2^{-2}	724	396	0.013097	2.57	0.007741	3.04	0.002864	3.53
2^{-3}	2498	1386	0.002275	2.52	0.001936	1.99	0.000391	2.87
2^{-4}	9738	5466	0.000484	2.23	0.000469	2.04	0.000049	2.99
2^{-5}	40230	22770	0.000099	2.28	0.000111	2.06	0.000005	3.13

6. Numerical illustration. We now illustrate our theoretical results by a simple numerical example.

6.1. Test problem. As computational domain for our tests, we choose $\Omega = \Omega_1 \cup \Omega_2$, where $\Omega_1 = (-1,1) \times (-1,0)$ and $\Omega_2 = \{(x,y) : x^2 + y^2 < 1 \text{ and } y \geq 0\}$. The exact pressure and conductivity matrix are defined as in [30] by

$$p(x,y) = \sin(\pi x)\sin(\pi y) \qquad \text{and} \qquad \mathcal{K}(x,y) = \begin{pmatrix} 4 + (x+2)^2 + y^2 & 1 + \sin(xy) \\ 1 + \sin(xy) & 2 \end{pmatrix},$$

and we set $u = -\mathcal{K}\nabla p$. These functions fulfill all regularity assumptions made throughout this manuscript, so we expect to observe the full convergence rates. We then partition Ω_1 into triangles and Ω_2 into rectangles in a conforming way, i.e., such that no hanging nodes are present at the interface. Although the domain is not exactly covered by the mesh, we still observe optimal convergence rates in our numerical tests.

6.2. Second-order approximation. We consider the approximation in RT_1-P_1 for triangles and BDFM_2-P_1 for parallelograms. Following the results of section 4, we here expect second-order convergence for the velocity and pressure and third-order convergence for the projected pressure. The results of our computations are depicted in Table 1. Recall that our method is restricted to affine elements. Using distorted parallelograms would severely impact the convergence rates. The predicted convergence rates are observed in our numerical tests. A graphical presentation of the solution is given in Figure 6.
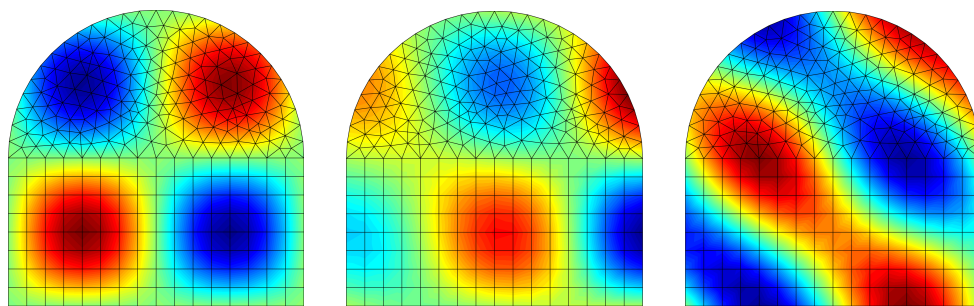
FIG. 6. *Snapshots of the pressure p_h (left) and the two velocity components $u_{x,h}$, $u_{y,h}$ (middle, right) for the second-order approximation.*

TABLE 2

Degrees of freedom, absolute discretization errors comparing the exact and lumped mixed methods, and estimated orders of convergence (eoc) for the errors presented.

h	DOF u	DOF p	$\|u_h - \widehat{u}_h\|$	eoc	$\|p_h - \widehat{p}_h\|$	eoc	$\|\pi_h^0(p_h - \widehat{p}_h)\|$	eoc
2^{-1}	164	84	1.621232	—	0.076209	—	0.037442	—
2^{-2}	724	396	0.318497	2.34	0.008252	3.20	0.003160	3.56
2^{-3}	2498	1386	0.047883	2.73	0.001895	2.12	0.000287	3.45
2^{-4}	9738	5466	0.007562	2.66	0.000460	2.04	0.000030	3.21
2^{-5}	40230	22770	0.001363	2.47	0.000109	2.06	0.000003	3.08

6.3. Comparison with exact mixed solution. Although similar convergence rates are attained in comparison to the exact mixed solution, it is interesting to quantify the absolute error in comparison to the standard mixed finite element solutions $\widehat{u}_h$ and $\widehat{p}_h$. The results are presented in Table 2. We note that the convergence rates are similar to those when comparing to the analytical solution (see Table 1), and no additional superconvergence is observed.

7. Discussion. In this paper, we extended the multipoint flux mixed finite element method of Wheeler and Yotov [30] to second-order elements and hybrid meshes in two and three space dimensions. The conditions for our abstract convergence theory were verified by construction of suitable finite elements and quadrature rules for various element types. Appropriate basis functions were defined that lead to block-diagonal mass matrices for the $H(\mathrm{div})$ variable. Our theory only covers elements stemming from affine transformations, while the extension to *slightly perturbed* parallelograms or parallelepipeds can be achieved by using similar arguments to those in [30]. The extension to distorted quadrilaterals and hexahedra is more involved; see [29].

Another way of efficiently solving saddle point types of problems is by means of hybridization, where the $H(\mathrm{div})$ continuity is transferred to a Lagrange multiplier. The new system can then be reduced to solve just for the newly introduced Lagrange variable. Subsequently, the pressure and velocity variables can be recovered locally by solving small systems. In comparison to hybridization, the multipoint flux method seems to lose even for the lowest-order BDM_1-P_0 pair. Indeed, as mentioned in [30], the size of the algebraic system is smaller, yet the size of the stencils is larger by a factor of about 3, which severely impacts the computational cost. The second-order method we present for triangles produces algebraic systems of similar size compared to hybridization, but the size of the stencils is larger by a factor of about 4. One
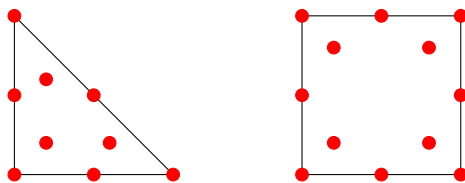
FIG. 7. *Location of quadrature points for third-order elements. Two degrees of freedom are associated to each quadrature point.*

TABLE 3
Quadrature points and weights for the unit triangle (left) and the unit square (right). Because of symmetry, only one point of each equivalence class is specified.

Nodes	n	Weights	Parameters	Nodes	n	Weights	Parameters
$\{(0,0)\}$	3	$\frac{1}{360}(14-\sqrt{7})$	—	$\{(0,0)\}$	4	$\frac{4}{225}$	—
$\{(\frac{1}{2},0)\}$	3	$\frac{1}{45}(1+\sqrt{7})$	—	$\{(\frac{1}{2},0)\}$	4	$\frac{2}{45}$	—
$\{(\alpha,\alpha)\}$	3	$\frac{7}{360}(14-\sqrt{7})$	$\frac{1}{21}(7-\sqrt{7})$	$\{(\alpha,\alpha)\}$	4	$\frac{169}{900}$	$\frac{1}{26}(13-\sqrt{39})$

upside is that with the multipoint flux method, no additional local computations are required to recover the pressure variable.

Another interesting field of application for mass lumping is the modeling of acoustic wave equations, e.g.,

$$\partial_t u + \nabla p = 0 \qquad \text{in } \Omega \times (0,T),$$
$$\partial_t p + \operatorname{div} u = 0 \qquad \text{in } \Omega \times (0,T),$$

by mixed finite element approximation in $H(\operatorname{div})$-L^2. Here, the hybrid method is not advantageous since it requires the solution of linear systems at each time step. The mass lumped variant does not require these additional computations. For the first-order method, we conducted an analysis for the acoustic wave propagation in [14]. We refer the reader to [12, 15] for more results in this direction.

Before closing, let us briefly review the basis construction principles underlying our approach and illustrate the possible extension to higher orders. We explicitly discuss elements for triangles and quadrilaterals of order $k+1=3$.

Step 1. We begin by specifying appropriate quadrature rules: We choose one quadrature point for every vertex and $k-1=1$ quadrature points for every edge. Additional quadrature points are chosen in the interior of the element to obtain a high order of exactness of the corresponding quadrature rule. The quadrature points of third-order elements in two dimensions are depicted in Figure 7, and the corresponding weights are defined in Table 3. These quadrature rules are exact for polynomials of order $p=4$ on triangles and order $p=5$ on the quadrilateral.

Step 2. Exactly two velocity degrees of freedom are associated with each quadrature point. The resulting local approximation spaces for the velocity are defined as

$$\widehat{V} = \operatorname{RT}_2^+(\widehat{T}) = \operatorname{RT}_2(\widehat{T}) \oplus B(\widehat{T}) \qquad \text{and} \qquad \widehat{V}^* = \operatorname{BDM}_2(\widehat{T})$$

for the reference triangle with $B(\widehat{T}) = \operatorname{span}\{\Phi_i,\ i=1,\dots,3\}$ with

$$\Phi_1(x,y) = x^2(xy, y^2-y), \quad \Phi_2(x,y) = y^2(xy, y^2-y), \quad \Phi_3(x,y) = y^2(x^2-x, xy),$$

and for the reference quadrilateral, we choose

$$\widehat{V} = \mathrm{BDFM}_3^+(\widehat{T}) = \mathrm{BDFM}_3(\widehat{T}) \oplus B(\widehat{T}) \qquad \text{and} \qquad \widehat{V}^* = \mathrm{BDFM}_3(\widehat{T})$$

with $B(\widehat{T}) = \mathrm{span}\{\Phi_i,\ i = 1, \ldots, 6\}$ with

$$\Phi_1(x,y) = x^2(x^2 - x, 0), \quad \Phi_2(x,y) = y^2(x^2 - x, 0), \quad \Phi_3(x,y) = xy(x^2 - x, 0),$$
$$\Phi_4(x,y) = y^2(0, y^2 - y), \quad \Phi_5(x,y) = x^2 y(x^2 - x, 0), \quad \Phi_6(x,y) = xy^2(x^2 - x, 0).$$

Note that $P_2(\widehat{T})^d \subset \widehat{V}$ and $P_2(\widehat{T}) \subset \mathrm{div}(\widehat{V})$ are required to guarantee the approximation properties of assumption (A4). The extension spaces $B(\widehat{T})$ consist of functions with independent divergences that also increase the divergence of the space $\widehat{V}^*$. Such functions can be obtained by choosing $H(\mathrm{div})$-bubble functions of sufficiently high order.

Step 3. Similar to section 5, the corresponding pressure spaces are defined by the divergence of the respective velocity spaces.

Let us note that the quadrature rules in our construction are somewhat nonstandard; in particular, the quadrature points on the quadrilateral do not have a tensor product structure. Unfortunately, we are not able to provide a systematic construction of quadrature rules for arbitrary orders yet. A similar issue was observed in [19]. In [3], multipoint-flux mixed finite elements of arbitrary order have been constructed for quadrilaterals and hexahedra based on tensor product Gauss–Lobatto quadrature points. More degrees of freedom are required for these elements, in comparison to ours, to obtain the same convergence rates, but the tensor product structure allows the systematic construction of elements of arbitrary order. Another way of constructing high-order approximations for elliptic problems with discontinuous pressure spaces is provided by discontinuous-Galerkin methods.

REFERENCES

[1] I. AAVATSMARK, T. BARKVE, O. BOE, AND T. MANNSETH, *Discretization on unstructured grids for inhomogeneous, anisotropicmedia.* I. *Derivation of the methods*, SIAM J. Sci. Comput., 19 (1998), pp. 1700–1716.

[2] I. AAVATSMARK, G. T. EIGESTAD, R. A. KLAUSEN, M. F. WHEELER, AND I. YOTOV, *Convergence of a symmetric MPFA method on quadrilateral grids*, Comput. Geosci., 11 (2007), pp. 333–345.

[3] I. AMBARTSUMYAN, E. KHATTATOV, J. LEE, AND I. YOTOV, *Higher order multipoint flux mixed finite element methods on quadrilaterals and hexahedra*, Math. Models Methods Appl. Sci., 29 (2019), pp. 1037–1077.

[4] T. ARBOGAST, M. F. WHEELER, AND I. YOTOV, *Mixed finite elements for elliptic problems with tensor coefficients as cell-centered finite differences*, SIAM J. Numer. Anal., 34 (1997), pp. 828–852.

[5] D. BOFFI, F. BREZZI, AND M. FORTIN, *Mixed Finite Element Methods and Applications*, Springer Ser. Comput. Math. 44, Springer, Heidelberg, 2013.

[6] F. BREZZI, *On the existence, uniqueness and approximation of saddle-point problems arising from lagrangian multipliers*, RAIRO Anal. Numer., 2 (1974), pp. 129–151.

[7] F. BREZZI, J. DOUGLAS, R. DURÁN, AND M. FORTIN, *Mixed finite elements for second order elliptic problems in three variables*, Numer. Math., 47 (1987), pp. 237–250.

[8] F. BREZZI, J. DOUGLAS, M. FORTIN, AND L. D. MARINI, *Efficient rectangular mixed finite elements in two and three space variables*, RAIRO Model. Math. Anal. Numer., 21 (1987), pp. 581–604.

[9] F. BREZZI, J. DOUGLAS, AND L. D. MARINI, *Two families of mixed elements for second order elliptic problems*, Numer. Math., 88 (1985), pp. 217–235.

[10] M. CARLSON, *Practical Reservoir Simulation*, PennWell Corporation, Tulsa, OK, 2006.

[11] P. G. CIARLET, *The Finite Element Method for Elliptic Problems*, North-Holland, Amsterdam, 1978.

[12] G. Cohen, *Higher-Order Numerical Methods for Transient Wave Equations*, Springer, Heidelberg, 2002.

[13] G. Cohen and P. Monk, *Gauss point mass lumping schemes for Maxwell's equations*, Numer. Methods Partial Differential Equations, 14 (1998), pp. 63–88.

[14] H. Egger and B. Radu, *A Mass-Lumped Mixed Finite Element Method for Acoustic Wave Propagation*, preprint, https://arxiv.org/abs/1803.04238, 2018.

[15] H. Egger and B. Radu, *A Mass-Lumped Mixed Finite Element Method for Maxwell's Equations*, preprint, https://arxiv.org/abs/1810.06243, 2018.

[16] A. Elmkies and P. Joly, *Éléments finis d'arête et condensation de masse pour les équations de Maxwell: Le cas 2D*, C. R. Acad. Sci. Paris Sér. I Math., 324 (1997), pp. 1287–1293.

[17] A. Elmkies and P. Joly, *Éléments finis d'arête et condensation de masse pour les équations de Maxwell: le cas de dimension 3*, C. R. Acad. Sci. Paris Sér. I Math., 325 (1997), pp. 1217–1222.

[18] A. Ern and J.-L. Guermond, *Theory and Practice of Finite Elements*, Appl. Math. Sci. 159, Springer-Verlag, New York, 2004.

[19] S. Geevers, W. Mulder, and J. van der Vegt, *New higher-order mass-lumped tetrahedral elements for wave propagation modelling*, SIAM J. Sci. Comput., 40 (2018), pp. A2830–A2857.

[20] K. Gröger and J. Rehberg, *Resolvent estimates in $W^{-1,p}$ for second order elliptic differential operators in case of mixed boundary conditions*, Math. Ann., 285 (1989), pp. 105–113.

[21] R. Ingram, M. F. Wheeler, and I. Yotov, *A multipoint flux mixed finite element method on hexahedra*, SIAM J. Numer. Anal., 48 (2010), pp. 1281–1312.

[22] R. A. Klausen and A. F. Stephansen, *Convergence of multi-point flux approximations on general grids and media*, Int. J. Numer. Anal. Model., 9 (2012), pp. 584–606.

[23] R. A. Klausen and R. Winther, *Robust convergence of multi point flux approximation on rough grids*, Numer. Math., 104 (2006), pp. 317–337.

[24] R. A. Raviart and J. M. Thomas, *Mathematical aspects of the finite element method*, in Lecture Notes in Math. 606, Springer, Berlin, 1987, pp. 292–315.

[25] R. Stenberg, *Postprocessing schemes for some mixed finite elements*, RAIRO Model. Math. Anal. Numer., 25 (1991), pp. 151–167.

[26] D. K. Todd and L. W. Mays, *Groundwater Hydrology*, Wiley, New York, 2004.

[27] M. Vohralik, *Equivalence between lowest-order mixed finite element and multi-point finite volume methods on simplicial meshes*, Math. Model. Numer. Anal., 40 (2006), pp. 367–391.

[28] M. Vohralik and B. I. Wohlmuth, *Mixed finite element methods: Implementation with one unknown per element, local flux expressions, positivity, polygonal meshes, and relations to other methods*, Math. Models Methods Appl. Sci., 23 (2013), pp. 803–838.

[29] M. Wheeler, G. Xue, and I. Yotov, *A multipoint flux mixed finite element method on distorted quadrilaterals and hexahedra*, Numer. Math., 121 (2012), pp. 165–204.

[30] M. F. Wheeler and I. Yotov, *A multipoint flux mixed finite element method*, SIAM J. Numer. Anal., 44 (2006), pp. 2082–2106.